Energetics and electronic structure of grain boundaries and surfaces of B- and H-doped Ni_3Al

Q. M. Hu,* R. Yang, D. S. Xu, Y. L. Hao, and D. Li
Titanium Alloy Laboratory, Institute of Metal Research, Chinese Academy of Sciences, 72 Wenhua Road, Shenyang 110016, China

W. T. Wu
State Key Laboratory for Corrosion and Protection, Institute of Metal Research, Chinese Academy of Sciences, 62 Wencui Road, Shenyang 110016, China

(Received 15 January 2003; published 20 June 2003)

By using a first-principles plane-wave pseudopotential method, the energetics and electronic structure of $\Sigma 5(210)$ grain boundary (GB) and the (210) surface of undoped as well as B- and/or H-doped Ni_3Al are investigated. The geometric structures of the GBs and surfaces are fully relaxed by minimizing the total energy and interatomic force. The results show that B induces a large lattice expansion but H does not. Both B and H ''prefer'' to occupy the Ni-rich hole at the GB or surface but not the Ni-deficient one. The segregation energies of B and H as well as the interaction energy between them at the GB and surface are calculated. The calculation indicates that B segregates more strongly to the GB than to the surface, which results in an increase in the Griffith work of the GB and, therefore, in agreement with the experiments, improves the ductility of Ni_3Al. Contrary to the case of B, H segregates more strongly to the surface than to the GB, which results in a decrease in Griffith work and confirms H as an embrittler for Ni_3Al. The calculation of the interaction energy between B and H demonstrates that B and H repel each other. Consequently, B may block the site of occupation of H at the GB, and restrain the H-induced embrittlement. To understand the mechanism of the obtained energetic features, the electronic densities of states (DOSs) are calculated. A comparison of the total DOSs between the B-doped GB and undoped as well as H-doped ones shows that B increases the hybridization of the GB, which contributes to the enhanced binding of the B-doped GB over the undoped and H-doped ones. When the site of B changes from bulk to GB to surface, the hybridization between B and Ni decreases accordingly. It is proposed that the segregation behavior of B at the GB and surface is dominated by the competition between B(p)–Ni(d) bond energy and the strain energy induced by B. The preference of B for the Ni-rich interstice in Ni_3Al is explained by the repulsive interaction between B and Al atoms resulting from the hybridization between their electrons when they are close to each other. The repulsion between B and H can also be explained by the same electronic structure mechanism as that for the B-Al interaction. The segregation of B at surface shifts the DOS of its nearest neighbor Ni to lower energy. This may increase the chemisorption potential energy of H_2O on Ni_3Al surface and, therefore, decrease the reactivity of the surface, inhibiting the environmental embrittlement of Ni_3Al.

DOI: 10.1103/PhysRevB.67.224203 PACS number(s): 68.35.−p, 68.35.Dv, 71.20.Gj, 81.40.Lm

I. INTRODUCTION

Stoichiometric Ni_3Al is ductile as a single crystal,[1] but it exhibits brittle intergranular fracture in the polycrystalline state.[2] Two factors have been proposed to account for the intergranular fracture: (1) environmental embrittlement (EE) due to hydrogen released from simple environments such as air and water at ambient temperature[3,4] in the process of surface reaction $M+H_2O \rightarrow M-O+2H$ or $M+H_2O \rightarrow M-OH+H$; and (2) an intrinsic weak link at the grain boundaries (GBs) as demonstrated by the fact that the fracture mode of polycrystalline Ni_3Al is always intergranular regardless of the atmosphere.[5,6] To overcome the embrittlement of the compound, microalloying and macroalloying strategies have been adopted. It is well documented that the addition of boron suppresses the brittleness of polycrystalline Ni_3Al and changes the brittle intergranular to ductile transgranular fracture.[2,7]

Attempts have been made to relate the intergranular fracture of Ni_3Al to the localized GB electronic structure by both experiments[8,9] and first-principles calculations.[10,11] It was suggested that the intrinsic weakness of GBs in Ni_3Al resulted from the less hybridization of GBs than bulk.[8,10] Muller *et al.*[8] measured the change in bonding at GBs using spatially resolved electron energy loss spectroscopy, and found that the Ni d band is less hybridized at GBs than in bulk material. Eberhart *et al.*[10] used a multiple-scattering X_α method to calculate the density of states (DOS) of a polyhedral model of a GB structure and compared it with the DOS of the corresponding single crystal. They found that more sp states appeared near the Fermi level in the DOS of the GB cluster. The increase in the DOS at the Fermi level for the grain boundary cluster actually indicates a weaker covalent bonding at the GB, which also means that there is a loss of hybridization at the GB. It was believed that the loss of hybridization at the GB will reduce the cohesive energy and increase the chemical activity of the GB, which may induce intergranular fracture.[8] In addition, Eberhart *et al.*[10] argued that the decrease in the covalent character of the bonds at the GB will make the GB more responsive to an external stimulus,[12] accommodate greater strain than the parent crystal and, therefore, lead to a localization of the strain and subsequently to intergranular fracture.[10,13,14]

The origin of the embrittling effect of H on Ni_3Al was

also approached by electronic structure calculations.[15–18] Sun *et al.*[15] investigated H-doped bulk Ni_3Al using a full-potential linear-muffin-tin-orbital (FP-LMTO) method. Their results show that hydrogen enhances the bonding charge directionality near some Ni atoms and reduces the interstitial charge, suggesting that the presence of H deteriorates local cohesion. Using a discrete-variational method within the framework of density-functional theory (DFT), Wang *et al.*[16] studied the behavior of H at a $\Sigma 13(320)$ tilt GB. Their calculations of local interatomic energy formulated by Wang *et al.*[17] indicate that H forms strong bonding with its nearest-neighbor Ni but bonds much weaker with its next-nearest-neighbor Ni atoms. Meanwhile, the bonding strength between host metal atoms neighboring H is weakened. The segregation of H at the GB induces a decrease in local charge density. On the basis of these results, they concluded that H acts as an embrittler in Ni_3Al and makes intergranular fracture easier. Using a full potential linearized-augmented plane-wave method (FLAPW), Lu *et al.*[18] calculated $\Delta E_{gb} - \Delta E_s$ due to H segregated at a $\Sigma 5$ tilt GB and at the surface of Ni_3Al, where $\Delta E_{gb} = E(gb+H) - E(gb)$ and $\Delta E_s = E(s+H) - E(s)$ are the hydrogen formation energies at the GB and at free surface, respectively. They obtained a positive value of 1.4 eV, indicating that H is an embrittler according to the theory of Rice and Wang.[19]

A number of mechanisms have been proposed to explain the beneficial effect of B on the ductility of Ni_3Al.[2,20–24] Efforts have also been made to understand the beneficial effect of B on the mechanical behavior of Ni_3Al on the basis of the electronic structure.[8,9,11,15,25–29] Painter and Averill[25] addressed the effect of B on the GB cohesion of pure Ni using a first-principles local spin-density atomic-cluster model. Their calculations showed that B is an enhancer of GB cohesion and increases the maximum sustainable restoring force in the cluster. Because B prefers to occupy the Ni-rich site in Ni_3Al,[15,30] the studies of the effect of B in pure Ni is instructive for the investigation of B effect in Ni_3Al. The calculation of Sun *et al.*[15] suggests that when bulk Ni_3Al is doped with B, the Ni(d) and B(p) hybridization between the nearest-neighbor Ni and B sites results in an enhancement of the intraplanar metallic bonding between the Ni atoms, an enhancement of interstitial bonding charge, and a reduction of the bonding charge directionality around the Ni atoms on the (001) planes, leading to B-induced strengthening. By spatially resolved electron energy loss spectroscopy measurement, Muller *et al.*[8] observed that, when B is present at a Ni-rich GB, the Ni(d) DOS resembles that of bulk Ni_3Al (less d holes at the Fermi level), supporting the argument that B improves the cohesion of GB. The interatomic energy calculations of Wang *et al.*[28] using a discrete-variational method show that B forms stronger bonding states with its neighboring host atoms, acting as a ''bridge'' and increasing the cohesive strength of the GBs in Ni_3Al.

The above first-principles investigations greatly extended our knowledge of the fracture of Ni_3Al. However, some fundamental problems, such as the segregation behavior and the electronic structure mechanism of B and H at the GB and surface, are still to be clarified. Experiments have shown that the addition of B affects the dissociation of H_2O on Ni_3Al surface,[31,32] which has not been interpreted theoretically. In addition, the above mentioned first-principles investigations are mostly based either on the local electronic structure, such as DOS and charge density, or on local interatomic interactions, which contributes indirectly to the fracture properties. Fracture properties are generally scaled by global energies such as the ''Griffith work.'' Therefore, to describe the GB fracture behavior more directly and clearly, it is desirable to investigate the energetics of the GB. Lu *et al.*[18] calculated the GB and surface energies of undoped and H-doped Ni_3Al using a FLAPW method, but did not present any results for B-doped case. Chen and co-workers[33,34] evaluated the GB and surface energy of undoped and B-doped Ni_3Al by atomic simulation using interatomic potentials; however, the energetics for the H-doped case was not presented. Though the atomic simulations (utilizing an interatomic potential) that involve the process of fitting parameters determine the energetics for GB accurately, they fail to provide insight into the chemical bonding characteristics. To our knowledge, the combined effect of B and H on the energetics of the GB and surface of Ni_3Al has not been studied.

In this paper, we investigate the energetics of the undoped and B and/or H modified GB and surface on an equal theoretical footing. The segregation energy of B and H at GB and surface as well as the Griffith works of pure and B and/or H modified GBs were presented. The geometric and electronic structure characteristics of the GB and surface are investigated. From the calculated electronic structure, some insights concerning the mechanism of B segregation at GB and surface, the origin of site occupancy of B in Ni_3Al, the mechanism of B–H interaction, and the effect of B on the reactivity of the surface of Ni_3Al, are obtained.

The paper is organized as follows. In Sec. II, we describe the models of GB and surface and the first-principles pseudopotential method used in our calculations. Section III presents the optimized GB and surface geometries. In Sec. IV, the segregation energies of B and H and the interaction energy between them at the GB and surface are evaluated. The effect of the doping of B and/or H on the Griffith work of the GB is estimated. In Sec. V, the behaviors of B and H in Ni_3Al are discussed on the basis of the calculated DOSs.

II. CALCULATION DETAIL

A. Method of calculation

To investigate the energetics as well as electron structural and geometric characteristics of B and/or H modified GB and surface of Ni_3Al, the CASTEP program, an implementation of the first-principles plane-wave pseudopotential method[35,36] based on density functional theory, is used. The local density approximation (LDA) is adopted to formulate the exchange-correlation potential.

The ultrasoft pseudopotentials[37] represented in reciprocal space with the Cepeley-Alder exchange-correlation potential were used for all elements involved in this work. The pseudopotential of Ni was generated with a nonlinear core correction. These pseudopotentials are provided with the CASTEP package[36] and have been well tested. Here, we present a simple test on the pseudopotentials of Ni and Al for

TABLE I. A simple test of the ultrasoft pseudopotentials of Ni and Al for Ni_3Al.

	Current work	TB-LMTO (Ref. 38)	AE-LMTO (Ref. 39)	Expt. (Refs. 38 and 39)
Lattice constant (Å)	3.49	3.51	3.55	3.57
Heat of formation (eV/atom)	2.27	2.20	1.94	1.59~1.62
Bulk modulus (Mbar)	2.20	1.46	2.10	2.40

Ni_3Al. Table I compares the equilibrium lattice constant, heat of formation, and bulk modulus evaluated by the first-principles plane-wave pseudopotential method used in the current work with those calculated by tight-binding linear muffin-tin orbital (TB-LMTO) (Ref. 38) and AE-LMTO (all electron linear muffin-tin orbital) (Ref. 39) methods and with experimental results referred to in Refs. 38 and 39. The lattice constant and heat of formation calculated here are close to those calculated by the TB-LMTO, but slightly different from those calculated by the AE-LMTO. However, it is interesting to note that the bulk modulus calculated here is close to that calculated by the AE-LMTO and the experimental measurement, but deviates considerably from that calculated by the TB-LMTO. The error of lattice constant calculated here relative to the experimental result is about 2%, in the range of the accuracy of the LDA. All the theoretical heats of formation are comparable to the experimental result.

In our calculations, the cutoff energy of plane waves (PWs), E_{cut}, is set at 330 eV. A finite basis set correction[41] is applied in the evaluation of energy and stress. The Pulay scheme of density mixing[40] is used for self-consistent field (SCF) calculation. The SCF tolerance is set at 1×10^{-6} eV.

B. Models of grain boundary and surface

In the current work, a supercell approach is used to construct the models of the GB and surface. The grain boundary of $\Sigma5(210)$ is constructed by means of the coincidence site lattice model as shown in Fig. 1(a) in which one supercell contains two GBs. With nine atomic layers in between, the interaction between two adjacent GBs is expected to be sufficiently weak. The composition of the GBs is 100/50, indicated by the composition of the first layer of each grain (percentage of Ni atoms: top grain/bottom grain).[33] There are two types of GB holes, one with all Ni neighbors (Ni-rich, site 1) and the other with both Ni and Al neighbors (Ni-deficient, site 2). The (210) surface is simulated by a slab model with ten (210) atomic layers and ten layers of vacuum in between, as shown in Fig. 1(b). The slab contains two surfaces: one containing 50% Ni and the other containing 100% Ni, corresponding to the composition of the GB. Similar to the GB, there are also two types of surface holes. For the impurity doped GB and surface, B and H are first placed nominally in the GB and surface holes, site 1 and/or site 2. For a consideration of the symmetry, the supercell with GBs is doped with two impurity atoms partitioned to the two GB planes. All atomic positions in the undoped and B and/or H doped supercells have been relaxed according to the total energy and force using the BFGS scheme, with lattice constants fixed at theoretical values as listed in Table I. The total energy and force tolerances for the geometry optimization are set at 1×10^{-5} and 0.03 eV/atom, respectively.

III. GEOMETRIC STRUCTURE

When the equilibrium structures are achieved, the B and H at site 1 and B at site 2 do not move far from their original sites. But it is interesting to note that the H atom originally placed at the Ni-deficient hole (site 2) moves to a distorted Ni-rich octahedral interstice (site 3) of the GB and the corresponding Ni-rich hole of the surface.

Table II lists the calculated atomic displacements obtained by subtracting the unrelaxed atomic positions normal to the boundary plane from the relaxed atomic positions. Positive values mean that the atom moves away from the GB plane, whereas negative ones mean that the atom moves closer to the GB plane. The data in the parentheses are the atomic displacements calculated by Lu *et al.*[18] It is seen that the displacements of the atoms in the first layer calculated in this work are comparable to those obtained by Lu *et al.* However, the displacements of the atoms in the second and third layers calculated here are significantly different from those calculated by Lu *et al.*, which may be related to the fact that they used a slab GB model, different from the supercell GB model used here. In spite of the discrepancy, both calculations show an oscillatory pattern of interlayer distance, that is, the first and third layers move away from and the second layer moves toward the GB planes.

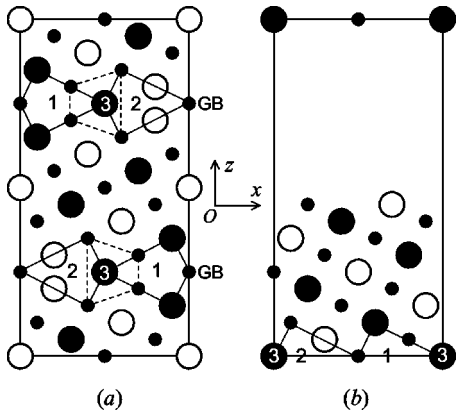

FIG. 1. Unrelaxed supercell geometry for (a) two $\Sigma5(210)$ tilt grain boundaries and (b) the (210) surface of Ni_3Al. The solid and open circles denote Ni and Al atoms, respectively. The large and small circles represent atoms on two adjacent (001) planes. Site 1 and the atoms represented by the large circles are located on the same (001) plane whereas the small circles, and sites 2 and 3 are on the (001) plane next to it.

TABLE II. Calculated atomic displacements (in Å) normal to the GB, for three (210) layers which are nearest to the $\Sigma 5(210)$ GB plane of Ni_3Al. B1 denotes the configuration of GB with a B atom occupying site 1, and H1, B2, and H3 have similar meanings. The data in the parentheses are those from FLAPW calculations by Lu *et al.* (Ref. 18).

Layer	Atom	Undoped	B1	H1	B2	H3
1	Ni	0.27(0.31)	0.31	0.28	0.27	0.27
1	Al	0.40(0.43)	0.39	0.40	0.44	0.40
2	Ni1	−0.05(−0.10)	0.06	−0.01	−0.07	−0.03
2	Ni2	−0.02(−0.07)	−0.03	−0.00	0.15	0.03
3	Al	0.01(0.17)	0.06	0.02	0.01	0.03
3	Ni	0.07(0.09)	0.07	0.08	0.11	0.07

As seen from Table II, the GB hole accommodating the B atom is obviously expanded. The displacements of Ni and Al atoms of the first layer are 0.27 and 0.40 Å, respectively, for the undoped system. The B atom at site 1 increases the displacement of its nearby Ni atom (at the first layer) from 0.27 to 0.31 Å, and the B atom at site 2 increases that of its nearby Al atom from 0.40 to 0.44 Å. However, the positions of the atoms near the H atom are almost not altered, meaning that H does not induce large lattice distortion.

IV. ENERGETICS

In this section, we first define the energies involved in our calculations. The GB energy for the undoped system is evaluated by

$$E_{\mathrm{gb}}=\frac{1}{2S}[E(N,2\mathrm{gb})-E(N)], \tag{1}$$

where $E(N,2\mathrm{gb})$ is the total energy of the N-site supercell containing two GBs [see Fig. 1(a)], $E(N)$ is the total energy of an N-site supercell of bulk Ni_3Al, and $S=a\times b$ is the area of the GB plane with a and b being the supercell lattice constants along x and y directions, respectively. Surface energy for the undoped system is expressed by

$$E_{\mathrm{surf}}=\frac{1}{S}[E(N/2,2\mathrm{s})-E(N)/2], \tag{2}$$

with $E(N/2,2\mathrm{s})$ being the total energy of the $N/2$-site supercell containing two surfaces. It should be noted that the surface energy calculated here is the sum of that of the two surfaces with different composition [see Fig. 1(b)].

The GB energy for the impurity doped system and the segregation energies of impurity at GB are defined as

$$E^{\mathrm{i}}_{\mathrm{gb}}=\frac{1}{2S}[E(N+2\mathrm{i},2\mathrm{gb})-E(N+2\mathrm{i})] \tag{3}$$

and

$$\Delta E^{\mathrm{i}}_{\mathrm{gb}}=\frac{1}{2S}\{[E(N+2\mathrm{i},2\mathrm{gb})+E(N)]-[E(N+2\mathrm{i})+E(N,2\mathrm{gb})]\}, \tag{4}$$

respectively, where $E(N+2\mathrm{i},2\mathrm{gb})$ and $E(N+2\mathrm{i})$ are the total energies of the impurity-doped supercells of GB and bulk Ni_3Al, respectively. Previous investigations[15,30] demonstrated that both B and H prefer to occupy the Ni-rich octahedral interstices in bulk Ni_3Al. Therefore, in the present work, $E(N+2\mathrm{i})$ is calculated with B or H occupying the Ni-rich octahedral interstices. A negative $\Delta E^{\mathrm{i}}_{\mathrm{gb}}$ means that the impurity has a tendency toward segregation at the GB. Similarly, the impurity doped surface energy and impurity segregation energy at the surface are defined as

$$E^{\mathrm{i}}_{\mathrm{surf}}=\frac{1}{2S}[E(N+2\mathrm{i},2\mathrm{s})-E(N+2\mathrm{i})] \tag{5}$$

and

$$\Delta E^{\mathrm{i}}_{\mathrm{surf}}=\frac{1}{S}\{[E(N/2+\mathrm{i},2\mathrm{s})+E(N)/2]-[E(N+2\mathrm{i})/2+E(N/2,2\mathrm{s})]\}, \tag{6}$$

respectively. Here, we would like to mention that, in previous studies[18,34] of B and H doped GB and surface, the impurity formation energy was defined as $\Delta E^{\mathrm{i}}_{\mathrm{gb}}=E(N+\mathrm{i},\mathrm{gb})-E(N,\mathrm{gb})$ and $\Delta E^{\mathrm{i}}_{\mathrm{surf}}=E(N+\mathrm{i},\mathrm{s})-E(N,\mathrm{s})$, from which one cannot determine whether the impurity segregates to the GB and surface or not.

The Griffith work is defined as the work needed to cleave a crystal along the GB, and can be calculated as the difference between the GB and surface energies, i.e.,

$$E_{\mathrm{GW}}=E_{\mathrm{surf}}-E_{\mathrm{gb}} \tag{7}$$

for an undoped system, and

$$E^{\mathrm{i}}_{\mathrm{GW}}=E^{\mathrm{i}}_{\mathrm{surf}}-E^{\mathrm{i}}_{\mathrm{gb}} \tag{8}$$

for an impurity doped system, respectively. From the definitions of segregation energies and the impurity doped GB and surface energies as shown in Eqs. (3)–(6), it is easy to show that the difference in the Griffith work between the impurity doped and undoped systems,

$$\Delta E^{\mathrm{i}}_{\mathrm{GW}}=E^{\mathrm{i}}_{\mathrm{GW}}-E_{\mathrm{GW}}, \tag{9}$$

can be equivalently expressed as the difference between the segregation energies of the impurity to surface and GB, i.e.,

$$\Delta E^{\mathrm{i}}_{\mathrm{GW}}=\Delta E^{\mathrm{i}}_{\mathrm{surf}}-\Delta E^{\mathrm{i}}_{\mathrm{gb}}. \tag{10}$$

A positive $\Delta E^{\mathrm{i}}_{\mathrm{GW}}$ indicates that the work needed to cleave the GB doped with impurity is larger than that for the undoped system, and the impurity segregates more strongly to the GB than to the surface.

Table III lists the GB energy, surface energy, and Griffith work for the undoped system. Also listed in the table are those energies obtained by other methods. It is seen that all the energies calculated here are larger than those calculated by embedded atom method (EAM) (Ref. 34) and FLAPW (Ref. 18) methods. The E_{gb} calculated here is about twice as large as that from the EAM,[33] consistent with the finding of Wright and Atlas[42] who showed that the DFT grain-boundary

TABLE III. GB and surface energies and Griffith work of undoped Ni_3Al (in J/m^2).

Source	E_{gb}	E_{surf}	E_{GW}
Current work	2.12	5.91	3.79
FLAPW[18]	1.7	4.2	2.5
EAM[33]	1.2	4.3	3.1

and staking fault energies tend to be a factor of 2 larger than the EAM values, although the EAM provides a good description of structural properties. Apart from the difference between the supercell model of the GB used here and the slab model used by Lu *et al.*[18] the discrepancy between our calculations and those of Lu *et al.* is possibly related to the lattice constants which are set at experimental values in the work of Lu *et al.* but is set at theoretical equilibrium values in the present work.

Table IV lists the segregation energies of B and H at the GB and surface and the change of Griffith work due to the doping of B or H. As seen from the table, for systems with B occupying the Ni-rich holes (site 1), the segregation energy of B at the GB is more negative than that at surface, which induces an increment of Griffith work of 0.22 J/m^2 relative to the undoped system. This result indicates that the strength of the GB is enhanced by the doping of B, consistent with the well known experimental observations. For the systems with B occupying the Ni-deficient holes (site 2), we obtain a negative GB segregation energy and a positive surface segregation energy. The Griffith work is 0.29 J/m^2 larger than that of the undoped system, which seems to suggest that B may also enhance the strength of the Ni-deficient GB. However, it should be noted that the segregation energies of B at the Ni-rich hole of the GB (-0.84 J/m^2) and surface (-0.62 J/m^2) are much more negative than those at the Ni-deficient hole (-0.22 and 0.07 J/m^2 of the GB and surface, respectively). Therefore, the stable configurations of B-doped GB and surface are the ones with B occupying the Ni-rich hole instead of the Ni-deficient one, the electronic structure mechanism of which will be discussed in Sec. V. It can be expected that, with the increase of Al at the GB, the segregation energy of B at GB will become positive. That is, B will not segregate to an Al-rich GB. Accordingly, B can not enhance the binding of an Al-rich GB. This result confirms the Auger electron spectorscopy (AES) analyses which indicate that the decrease in ductility with increasing aluminum content of B-doped Ni_3Al was associated with a decreasing tendency for B segregation to the GB.[2,43]

TABLE IV. Segregation energies of B and H at GB (ΔE^i_{gb}) and surface (ΔE^i_{surf}) and change of Griffith work (ΔE^i_{GW}) due to the doping of B and H (in J/m^2).

Impurity	ΔE^i_{gb}	ΔE^i_{surf}	ΔE^i_{GW}
B at site 1	-0.84	-0.62	0.22
B at site 2	-0.22	0.07	0.29
H at site 1	0.17	-0.03	-0.20
H at site 3	-0.04	-0.29	-0.25

For H at site 1, we obtain a positive GB segregation energy (0.17 J/m^2) but a slightly negative surface segregation energy (-0.03 J/m^2), which means that H does not segregate to the Ni-rich GB hole but weakly segregates to the Ni-rich surface hole. For H at distorted octahedral interstices (site 3), we get a slightly negative GB segregation energy and a very negative surface segregation energy, indicating that H weakly segregates to site 3 of the GB and more strongly to the corresponding surface hole. The stronger segregation of H to the surface than to the GB results in a decrease in the Griffith work, and induces the hydrogen embrittlement of Ni_3Al, again in consistency with experimental findings.

The above results show the effects of B and H atoms on the Griffith work of the GB when they are not associated with each other. It is interesting to know what would happen if B and H coexist at the GB or surface. The calculated Griffith work of the system containing both B (site 1) and H (site 3) is 3.82 J/m^2, close to that of the undoped system (3.79 J/m^2), which is not adequate to explaining the transition of fracture mode from intergranular to transgranular induced by B doping. In fact, if considering the interaction between B and H, one finds that B and H cannot coexist at the GB or surface. The interaction energy between B and H at the GB or surface can be evaluated from

$$\Delta E = [E(\mathrm{B+H}) + E] - [E(\mathrm{B}) + E(\mathrm{H})], \tag{11}$$

where $E(\mathrm{B+H})$, $E(\mathrm{B})$, and $E(\mathrm{H})$ are the total energies of the GB or surface supercells containing both B (site 1) and H (site 3), B only, and H only, respectively. E is the total energy of the GB or surface supercell of undoped Ni_3Al. The calculated interaction energy is 0.17 eV for both the GB and surface, meaning that B and H repel each other at the GB or surface. Therefore, once B segregates to the GB or surface, the neighboring sites will be unavailable for H due to its repulsive interaction with B (because the segregation energy of B is much larger than that of H, the segregation of B has priority over that of H). Therefore, besides the beneficial effect of B in improving the binding strength of the GB, as shown earlier, the blocking of H site occupation by B also contributes to the enhancement of the GB, confirming the hypothesis of some experimental researchers.[23,24]

Both theoretical calculations[34] and experiments[44] demonstrated that B segregates to the GBs of Ni_3Al. However, previous theoretical investigation did not give direct information concerning the segregation behavior of B and H at the free surfaces.[18,34] Different from previous studies, our calculations explicitly give the segregation energies of B and H at the surface. A direct comparison between the theoretical and experimental results of surface segregation, however, is difficult because the theoretical calculation deals with an ideal surface that can hardly be obtained by experiment. Many factors, such as unwanted contaminants, imperfect surface structure, etc., may affect the behavior of surface segregation.[43–45] However, we do find some consistency between our calculations and experiments. As seen from Table IV, B segregates to the Ni-rich hole of surface but not to the Ni-deficient one. This result agrees with the experimental

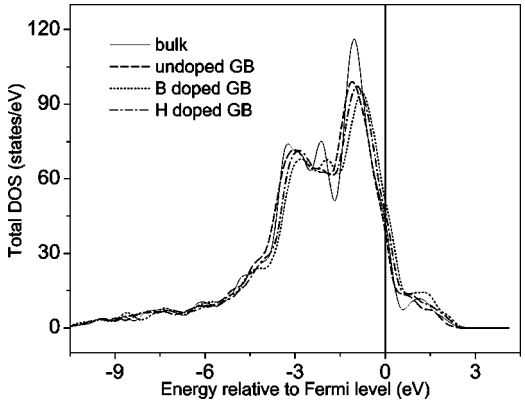

FIG. 2. Total density of states for bulk Ni_3Al, undoped GB, GB with B at site 1, and GB with H at site 3.

finding that B segregates significantly to a sputter etched Ni_3Al surface, where preferential removal of Al was observed but does not segregate strongly to well annealed surface that is fairly representative of the bulk alloy composition.[43]

V. ELECTRONIC STRUCTURE

In this section, we will explore the electronic structure mechanism underlying the behavior of B and/or H doped Ni_3Al. Figure 2 compares the total DOS of the supercells of bulk Ni_3Al and undoped and impurity-doped GB. The impurities occupy their stable sites at the GB (site 1 for B and site 3 for H). It is seen that, for the DOS of bulk Ni_3Al, a pseudogap occurs just above the Fermi level, and a peak exists at about -2.0 eV, which are the results of the hybridization between Ni(d) and Al(sp) states. For the GB supercell, the pseudogap above the Fermi level and the peak at -2.0 eV are invisible. This is because, for the GB supercell, the Ni atoms around site 1 have fewer nearest-neighbor Al atoms than the Ni in bulk whereas the Al atoms around site 2 have fewer nearest-neighbor Ni atoms than the Al in bulk (see Fig. 1). Therefore, the hybridization at GB is weakened, and more nonbonding states occur near the Fermi level (see Fig. 3 which shows the variation of DOS at the Fermi level

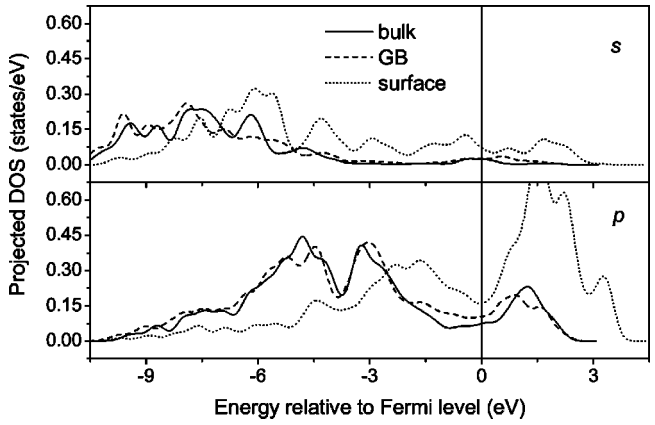

FIG. 3. Projected density of states of Al in bulk, near the GB plane, and near the surface plane.

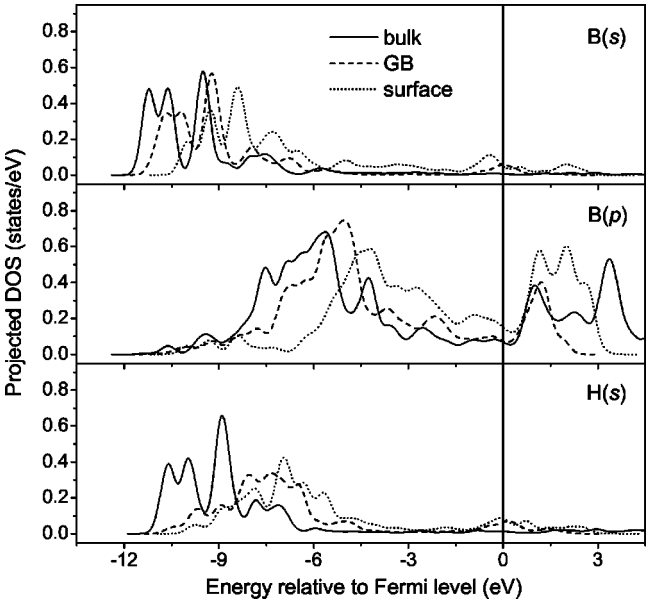

FIG. 4. Projected density of states of B and H in bulk Ni_3Al, in the GB and surface holes. In bulk Ni_3Al, both B and H occupy the Ni-rich octahedral interstice; at the GB and surface, B is located at site 1, and H occupies site 3 (see Fig. 1).

for Al in different environments). The weakening of hybridization represents a decrease in binding of GB relative to the bulk. For the B-doped GB, a peak near -2.0 eV and the pseudogap appears again, though the height of the peak and the depth of the pseudogap are somewhat smaller than those for the bulk Ni_3Al (Fig. 2). This is because B hybridizes with its nearest-neighbor Ni atoms, indicating a covalent bonding between B and Ni. The covalent bonding is responsible for the beneficial effect of B on the strength of GB. However, the DOS of a H-doped GB is very similar to that of an undoped GB. From the point of view outlined above, we conclude that H does not improve the cohesion of GB.

As discussed in Sec. IV, the effects of impurities on the intergranular fracture of Ni_3Al can be represented by the changes of Griffith work, which are in turn determined by the segregation behavior of impurities at the GB or surface. Therefore, it is of fundamental interest to understand the mechanism of the impurity segregation. It is natural to consider that the impurity segregation is related to the electronic structure of the systems. In order to explore the mechanism of the segregation behavior of the impurities, we calculated the projected DOSs of B and H in different environments[46] (Fig. 4).

Because the s states of B are pushed far below the Fermi level (see the top graph of Fig. 4), their contribution to the B-Ni binding is quite small for the B atoms in all three environments (bulk, GB, and surface). As a result of B(p)–Ni(d) hybridization, there are pseudogaps near the Fermi level for the p DOS of B that indicate covalent interaction between B and its surrounding Ni atoms (see the middle graph of Fig. 4). The DOS at the Fermi level, N_f, increases, but the width of the pseudogap decreases, from bulk to GB, then to surface, which means that the covalent interaction becomes weaker accordingly. This is because

from the octahedral interstice to the GB hole, then to the surface hole, the number of nearest-neighbor Ni atoms coordinated around B decreases. Therefore, considering only the covalent interaction, GB and surface holes are not preferred by B compared to the octahedral interstice in bulk. This seems to contradict the calculation of segregation energy that implies the segregation of B at the GB and surface. However, it should be noted that B doping induces a considerable amount of local lattice expansion (see Table II). Consequently, strain energy is needed for the accommodation of B, which induces an increase in the energy of the system. Therefore, the segregation behavior of B is actually the result of the competition between the B(p)–Ni(d) bond energy, E_{pd}, and the strain energy, E_{str}. Because the volume of the octahedral interstice in bulk Ni_3Al is smaller than that of the Ni-rich GB hole, and the surface hole is open whereas the GB hole is closed, the strain energy induced by B-doping decreases from bulk to the GB to surface. The segregation of B at the GB and surface may be explained by the fact that when B moves from the octahedral interstice in bulk to the GB or the surface hole, the decrease in strain energy, $E_{\mathrm{str}}^{\mathrm{bulk}}-E_{\mathrm{str}}^{\mathrm{GB}}$ or $E_{\mathrm{str}}^{\mathrm{bulk}}-E_{\mathrm{str}}^{\mathrm{surf}}$, is larger than the increment of energy due to the weakening of B(p)–Ni(d) bond, $E_{\mathrm{pd}}^{\mathrm{GB}}-E_{\mathrm{pd}}^{\mathrm{bulk}}$ or $E_{\mathrm{pd}}^{\mathrm{surf}}-E_{\mathrm{pd}}^{\mathrm{bulk}}$. Similarly, the stronger segregation of B to the GB than to surface stems from the fact $(E_{\mathrm{str}}^{\mathrm{GB}}-E_{\mathrm{str}}^{\mathrm{surf}})<(E_{\mathrm{pd}}^{\mathrm{surf}}-E_{\mathrm{pd}}^{\mathrm{GB}})$.

Similar to that of B, the s DOS of H is pushed far below the Fermi level due to the H(s)–Ni(d) hybridization (see the bottom graph of Fig. 4), and contributes little to the binding between H and Ni. However, different from the case of B, there is no p-d hybridization between H and Ni. In addition, as seen from Table II, H doping does not induce significant lattice expansion. Therefore, the mechanism of segregation of B at the GB and surface discussed above is not applicable to explaining the segregation behavior of H.

Though both experiment[30] and theoretical calculation[15] demonstrated that B and H prefer to occupy Ni-rich octahedral interstitial sites in Ni_3Al, the mechanism behind the preferential occupation was not fully explained. The top graph of Fig. 5 compares the projected DOSs of B at site 1 (without nearest neighbor Al) to those of B at site 2 (with two nearest neighbor Al atoms). It is seen that the p DOS of B at site 2 has three more peaks below about -7.5 eV than that of B at site 1, and a pseudogap occurs at about -7.0 eV. For the s DOS of B at site 2, there occurs a pseudogap located at about -10.5 eV. Similar features are seen in the projected DOSs of Al near the GB plane with and without a nearest neighbor B (see the bottom graph of Fig. 5). The occurrence of the additional low-lying states and pseudogaps in the projected DOSs of the nearest neighbor B and Al atoms relative to those of B and Al that are separated from each other can be explained as results of the hybridization between the electrons of Al and B. B(p)–Ni(d) and Al(p)–Ni(d) hybridizations result in the formation of bonding and antibonding states which are separated by the pseudogaps near the Fermi level (see the thin curves in Fig. 5) for B and Al, respectively. The bonding states due to B(sp)–Ni(d) and Al(sp)–Ni(d) hybridizations are of close

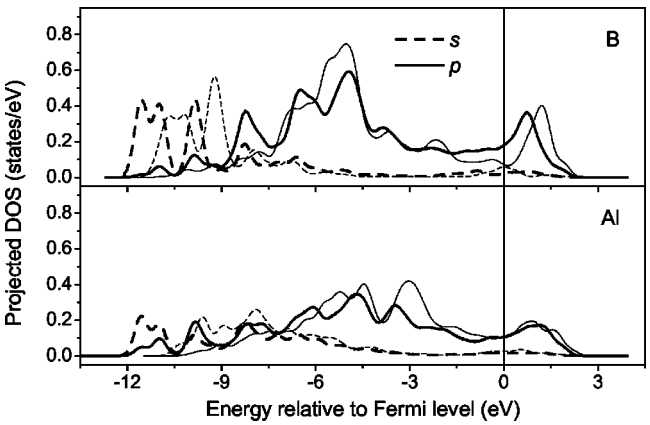

FIG. 5. Projected density of states of B and Al at GB. The top graph compares the DOSs of B at site 1 (thin curves) without nearest neighbor Al to those of B at site 2 (thick curves) with two nearest neighbor Al atoms. The bottom one shows the DOSs of Al with (thick curves) and without nearest neighbor B (thin curves).

energy levels and, therefore, they further hybridize when B and Al are nearest neighbors of each other, which induces the additional low-lying states and pseudogaps. As seen from Fig. 5, both the bonding and antibonding states resulting from the hybridization between the electrons of B and Al are below the Fermi level, and are occupied by electrons. Consequently, this hybridization contributes little to the binding between B and Al. However, the Pauli principle states that no two electrons can be in the same states, which means that the states of B have to become orthogonal to those of Al when they come into contact. This raises the kinetic energy and indicates the repulsion between B and Al, which explains the preference of B for the Ni-rich interstice in Ni_3Al. The electronic structure mechanism for the repulsion between B and Al seems always true for the interaction between two simple metal atoms in a transition metal host.[47,48]

The calculation of interaction energy between H and B atoms demonstrates that they repel each other (see Sec. IV), which can also be traced to the electronic interaction between H and B (see Fig. 6 for a comparison of the projected DOSs of B and H associated with each other with those of B and H separated from each other). The mechanism is similar to that of the interaction between B and Al as discussed above.

As shown in Sec. III, the H atom originally placed in the Ni-deficient hole (site 2) of the GB and surface moves to the distorted Ni-rich octahedral interstice (site 3) after the geometric optimization. This may also be the result of the repulsion between H and Al due to the same electronic mechanism as discussed above. Though B and Al atoms repel each other, different from the case of H, the B atom placed at site 2 does not move to site 3. This is understandable because H does not induce a significant lattice distortion but B expands the lattice considerably. The large strain energy needed to accommodate B at site 3 makes it inaccessible for B.

It is now widely accepted that the hydrogen released from simple environments such as air and water at ambient temperature in the process of surface reaction is responsible for the environmental embrittlement of Ni_3Al.[3,4] Therefore, it is

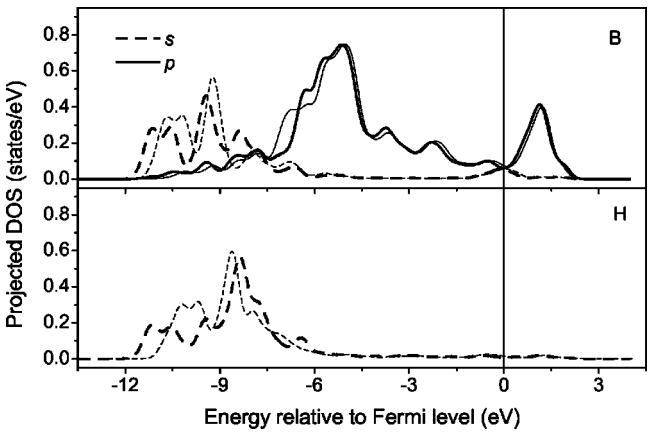

FIG. 6. Projected density of states of B and H at GB. The top graph compares the DOSs of B at site 1 with H at site 3 (thick curves) to those of B without H (thin curves). The bottom graph shows the DOSs of H at site 3 with (thick curve) and without (thin curve) B.

interesting to know if B doping affects the reactivity on the surface of Ni_3Al. It has been recognized that the reactivity is closely related to the electronic structure in the valence band of the metal surface. For transition and noble metal surfaces, the reactivities can be evaluated by the location and width of their *d* bands.[49,50] Moving to the left in the $3d$, $4d$, or $5d$ series of the Periodic Table, the *d* band moves up in energy, so that the metal is more reactive. Going down a column of the Periodic Table, the width of the *d* band increases, and the reactivity of the metal decreases accordingly. For a further discussion of this topic, see a recent review by Hammer and Norskov.[49]

The calculation of the segregation energy in Sec. IV shows that B does not segregate to the Al associated surface hole. So the change of reactivity of Ni_3Al surface due to B doping may be dominated by the variation of the electronic structure of Ni but not that of Al. Figure 7 compares the *d* partial DOSs of Ni at B-free and B-doped surface. It can be seen that the DOS of Ni neighboring B is shifted to a lower energy. This should increase the chemisorption potential energy of H_2O on the Ni_3Al surface, and, therefore, decrease the reactivity of the surface, inhibiting the environmental embrittlement of Ni_3Al. However, we also noted that, to explain the intergranular fracture of B-doped Ni_3Al at higher H_2 pressures, Cohron *et al.*[51] suggested that B possibly promotes the dissociation of molecular H_2 into atomic H at the Ni_3Al surface. This suggestion seems in disagreement with the calculations of the DOS presented above. It should be noted that the modification of DOS of Ni by B is just a

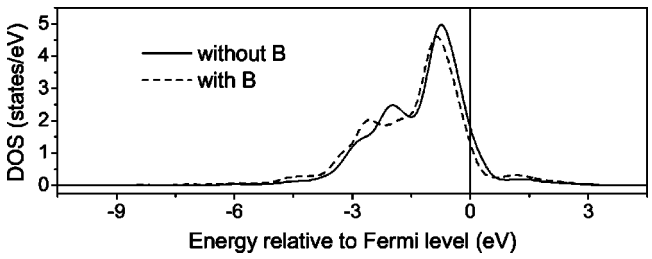

FIG. 7. Comparison of projected density of states (in states/eV) of Ni atoms at the surface of B-doped (dash curve) and B-free (solid curve) Ni_3Al.

starting point of the investigation of the effect of B on the surface reaction. A more elaborate and comprehensive theoretical investigation should be conducted in order to solve the problem.

VI. CONCLUSION

By using a first-principles pseudopotential method, the energetics and electronic structure of $\Sigma 5(210)$ grain boundary and (210) surface of undoped as well as B and/or H-doped Ni_3Al are investigated. The main results can be summarized as follows.

(1) B segregates more strongly to the GB than to the surface, resulting in an increase in the Griffith work for the GB fracture. Contrary to the case of B, H segregates more strongly to the surface than to the GB, which induces a decrease in Griffith work.

(2) The segregation behavior of B is determined by the competition between the change of the B-Ni bond energy and the change of strain energy with B in different lattice environments (bulk, GB, or surface).

(3) As a result of the hybridization between their electrons, B, H, and Al repel each other when one of them is the nearest neighbor of another, which explains the preference of B and H for the Ni-rich interstitial site in Ni_3Al.

(4) The beneficial effect of B on the ductility of Ni_3Al may originate from three contributions: (a) B bonding covalently to Ni at the GB, which enhances the binding of the GB; (b) B blocking the site of occupation of H at the GB due to the repulsive interaction between B and H and, therefore, inhibiting the H induced embrittlement; and (c) the segregation of B to the surface, decreasing the reactivity of the Ni_3Al surface and, therefore, hampering the decomposition of H_2O.

ACKNOWLEDGMENT

This work was supported by the Ministry of Science and Technology of China under Grant No. TG2000067105.

*Corresponding author. Email address: qmhu@imr.ac.cn

[1] N. S. Stoloff and C. T. Liu, *Physical Metallurgy and Processing of Intermetallic Compounds*, ed. N. S. Stoloff and V. K. Sikka, Chapman & Hall, New York, 1996. p. 159.

[2] C.T. Liu, C.L. White, and J.A. Horton, Acta Metall. **33**, 213 (1985).

[3] E.P. George, C.T. Liu, and D.P. Pope, Scr. Metall. Mater. **27**, 365 (1992).

[4] E.P. George, C.T. Liu, and D.P. Pope, Acta Mater. **44**, 1757 (1996).

[5] E.P. George, C.T. Liu, and D.P. Pope, Scr. Metall. Mater. **28**, 857 (1993).

[6] E.P. George, C.T. Liu, and D.P. Pope, Scr. Metall. Mater. **30**, 37 (1994).

[7] K. Aoki and O. Izumi, Nippon Kinzoku Gakkaishi **43**, 1190 (1979).
[8] D.A. Muller, S. Subramanian, P.E. Batson, S.L. Sass, and J. Silcox, Phys. Rev. Lett. **75**, 4744 (1995).
[9] S. Subramanian, D.A. Muller, J. Silcox, and S.L. Sass, Mater. Sci. Eng., A **239–240**, 297 (1997).
[10] M.E. Eberhart and D.D. Vvedensky, Phys. Rev. Lett. **58**, 61 (1987).
[11] J.R. Alvarez and P. Rez, Acta Mater. **49**, 795 (2001).
[12] R. Haydock, J. Phys. C **14**, 3807 (1981).
[13] E.M. Schulson, D.L. Davidson, and D. Viens, Metall. Trans. A **14**, 1523 (1983).
[14] S. Hanada, T. Ogura, S. Watanabe, O. Izumi, and T. Masumoto, Acta Metall. **34**, 13 (1986).
[15] Sheng N. Sun, Nicholas Kioussis, Say-Peng Lim, A. Gonis, and William H. Gourdin, Phys. Rev. B **52**, 14 421 (1995).
[16] Wang Fuhe and Wang Chongyu, Phys. Rev. B **57**, 289 (1998).
[17] C.Y. Wang, F. An, B.L. Gu, F.S. Liu, and Y. Chen, Phys. Rev. B **38**, 3905 (1988).
[18] Gang Lu, Nicholas Kioussis, R. Wu, and Mikael Ciftan, Phys. Rev. B **59**, 891 (1999).
[19] James R. Rice and Jian-Sheng Wang, Mater. Sci. Eng., A **107**, 23 (1989).
[20] E.M. Schulson, T.P. Weihs, J. Baker, H.J. Frost, and J.A. Horton, Acta Metall. **34**, 1395 (1986).
[21] T.K. Chaki, Philos. Mag. Lett. **61**, 5 (1990).
[22] T.K. Chaki, Philos. Mag. Lett. **63**, 123 (1991).
[23] T. Takasugi, K. Hono, S. Suzuki, S. Hanada, and T. Sakurai, Scr. Metall. Mater. **29**, 1587 (1993).
[24] X.J. Wan, J.H. Zhu, K.L. Jing, and C.T. Liu, Scr. Metall. Mater. **31**, 677 (1994).
[25] G.S. Painter and F.W. Averill, Phys. Rev. Lett. **58**, 234 (1987).
[26] Sheng N. Sun, Nicholas Kioussis, and Mikael Ciftan, Phys. Rev. B **54**, 3074 (1996).
[27] G.S. Painter, C.L. Fu, and F.W. Averill, J. Appl. Phys. **81**, 2135 (1997).
[28] Wang Fuhe, Wang Chongyu, and Yang Jinlong, J. Phys.: Condens. Matter **8**, 5527 (1996).
[29] Fu-He Wang, Jia-Xiang Shang, Jia-Ming Li, and Chong-Yu Wang, Intermetallics **8**, 589 (2000).
[30] N. Masahashi, T. Takasugi, and O. Izumi, Acta Metall. **36**, 1815 (1988).
[31] Jinliu Wang and Yip-Wah Chung, Intermetallics **9**, 349 (2001).
[32] Jinliu Wang and Yip-Wah Chung, J. Phys. Chem. B **104**, 3219 (2000).
[33] S.P. Chen, A.F. Voter, and D.J. Srolovitz, Scr. Metall. **20**, 1389 (1986).
[34] S.P. Chen, A.F. Voter, R.C. Albers, A.M. Boring, and P.J. Hay, J. Mater. Res. **5**, 955 (1990).
[35] M.C. Payne, M.P. Teter, D.C. Allan, T.A. Arias, and J.D. Joannopoulos, Rev. Mod. Phys. **64**, 1045 (1992).
[36] M.D. Segall, Philip J.D. Lindan, M.J. Probert, C.J. Pickard, P.J. Hasnip, S.J. Clark, and M.C. Payne, J. Phys.: Condens. Matter **14**, 2717 (2002).
[37] D. Vanderbilt, Phys. Rev. B **41**, 7892 (1990).
[38] P. Ravindran, G. Subramoniam, and R. Asokamani, Phys. Rev. B **53**, 1129 (1996), and references therein.
[39] J.-h Xu, B.I. Min, A.J. Freeman, and T. Oguchi, Phys. Rev. B **41**, 5010 (1990), and references therein.
[40] P. Pulay, Mol. Phys. **17**, 197 (1969).
[41] G.P. Francis and M.C. Payne, J. Phys.: Condens. Matter **2**, 4395 (1990).
[42] Alan F. Wright and Susan R. Atlas, Phys. Rev. B **50**, 15 248 (1994).
[43] C.L. White, C.T. Liu, and R.A. Padgett, Acta Metall. **36**, 2229 (1988), and references therein.
[44] C.L. White, R.A. Padgett, C.T. Liu, and S.M. Yalisove, Scr. Metall. **18**, 1417 (1984).
[45] D.T.L. van Agterveld, S.A. Koch, G. Palasantzas, and J.T.M. De Hosson, Surf. Sci. **482**, 254 (2001).
[46] The calculation of the projected DOS in CASTEP is performed using a projection of the PW states onto a localized basis using a technique described by D. Sanchez-Portal *et al.* [Solid State Commun. **95**, 685 (1995)]. The eigenstates $\psi_\alpha(\mathrm{k})$ obtained from the PW calculation when sampling at a given wave vector **k** are projected onto Bloch functions formed from a linear combination of atomic orbitals basis set $\phi_\mu(\mathrm{k})$. The basis set is chosen as the pseudoatomic orbitals, generated from the pseudopotentials used in the electronic structure calculation. The orbitals are calculated by solving for the lowest energy eigenstates of the pseudopotential in a sphere, using a spherical Bessel basis set.
[47] Q.M. Hu, D.S. Xu, R. Yang, D. Li, and W.T. Wu, Phys. Rev. B **66**, 064201 (2002).
[48] Q.M. Hu, D.S. Xu, R. Yang, D. Li, and W.T. Wu, Philos. Mag. **83**, 217 (2003).
[49] B. Hammer and J.K. Norskov, Adv. Catal. **45**, 71 (2000).
[50] B. Hammer and J.K. Norskov, Surf. Sci. **343**, 211 (1995).
[51] J.W. Cohron, E.P. George, L. Heatherly, C.T. Liu, and R.H. Zee, Acta Mater. **45**, 2801 (1997).